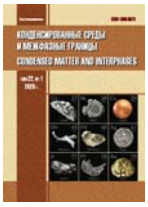

Condensed Matter and Interphases
(Kondensirovannye sredy i mezhfaznye granitsy)

**Original articles**

DOI: https://doi.org/10.17308/kcmf.2020.22/2526 eISSN 2687-0711
Received 11 January 2020
Accepted 15 February 2020
Published online 25 March 2020

# Synthesis, Structure and Magnetic Properties of Cobalt-Zinc Nanoferrite for Magnetorheological Liquids

**© 2020 Yu. S. Haiduk✉[a], E. V. Korobko[b], K. A. Shevtsova[b], D. A. Kotsikau[a], I. A. Svito[a], A. E. Usenka[a], D. V. Ivashenko[a], A. Fakhmi[c], V. V. Pankov[a]**

[a]*Belarusian State University, 4 Nezalezhnastsi av., Minsk 220030, Republic of Belarus*

[b]*A. V. Luikov Heat and Mass Transfer Institute of the National Academy of Science, 15 P. Brovki str., Minsk 220072, Republic of Belarus*

[c]*University of Applied Sciences Marie Curie-Strasse 1D-47533 Kleve, Federal Republic of Germany*

**Abstract**

An upcoming trend in the application of micro- and nanosized magnetic particles is the development of magnetorheological fluids for the automatic systems of damping devices in which the particles play the role of a component in the complex dispersed phase. In the search for magnetic materials for magnetorheological fluids, the most important criteria in choosing are high shear stress of the suspension based on the particles vs. applied magnetic field and a low value of coercive force. The aim of the work was to investigate the structure, morphology, and magnetic properties of the nanoscaled powders of Co, Zn-ferrites and the evaluation of their effectiveness upon the rheological properties of the developed magnetorheological fluids.

The Co, Zn-ferrite nanopowderwas synthesized by spray-drying technique followed by heat treatment in the presence of the inert matrix. The features of its morphology were investigated by x-ray diffraction analysis, transmission electron microscopy, and IR-spectroscopy.

The powdered nanoferrite $Co_{0.65}Zn_{0.35}Fe_2O_4$, used as a filler of magnetic fluids, demonstrated values of coercive force $H_c$ (10 K) = 10.8 kOe, $H_c$ (300 K) = 0.4 kOe as well as relative residual magnetization $M_r/M_s$(10 K) = 0.75, $M_r/M_s$(300 K) = 0.24. The proposed synthesis technique allows obtaining crystallized particles of the ferrite with sizes not larger than 50 nm, which possess high shear stress in magnetorheological suspensions.

The synthesis technique allows controlling the magnetic properties of Co,Zn-ferrite (as a component of magnetorheological suspensions) by non-magnetic double-charged ion substitution of $Co^{2+}$, i.e. ions $Zn^{2+}$, in Co,Zn-spinel has been developed. The possibility has been established to decrease the coercive force and increase the magnetization up to the maximum cobalt content, corresponding to the composition formulae $Co_{0.65}Zn_{0.35}Fe_2O_4$. The high value of shear stress ($10^3$ Pa) at a relatively low value of magnetic induction (600 mT and higher) makes the material applicable as a filler for the magnetorheological suspensions of damping devices.

**Keywords:** cobalt zinc ferrite, magnetorheological liquids, magnetic nanoparticles.

***For citation:*** Haiduk Yu. S., Korobko E. V., Shevtsova K. A., Kotikov D. A., Svito I. A., Usenka A. E., Ivashenko D. V., Fakhmi A., Pankov V. V.Synthesis, structure, and magnetic properties of cobalt-zinc nanoferrite for magnetorheological liquids. *Kondensirovannye sredy i mezhfaznye granitsy = Condensed Matter and Interphases*. 2020; 22 (2):28–38. DOI: https://doi.org/10.17308/kcmf.2020.22/2526

## 1. Introduction

A promising area for the application of micro- and nanosized magnetic particles is the creation of magnetorheological fluids (MRF) for controlled hydraulic automation devices in which such particles are a component of the complex dispersed phase [1, 2]. Such liquids are used as an active medium for damping devices designed for the protection of vehicles, industrial equipment, buildings, and structures from vibrations and other mechanical influences, as well as for the

✉ Yulyan S. Haiduk, e-mail: j_hajduk@bk.ru

manufacture of various sensors, measuring elements, electromechanical converters, targeted drug delivery, and the diagnosis of diseases in biology and medicine [3–5].

Objects sensitive to the magnetic field can be obtained based on fluid compositions with dispersed solid-phase fillers possessing magnetic properties. In the presence of an external magnetic field, strong particle structural bonds are formed along the magnetic field vector in such compositions, leading to an increase in the viscosity of the compositions and is a necessary condition for creating controlled damping devices.

The magnetic properties of nanopowders, which can be components of these fluid compositions, are determined by the chemical composition, type of crystal lattice, degree of its defectiveness, particle size and shape, morphology (for structurally inhomogeneous particles), and the degree of interaction of the particles with the surrounding liquid and other particles. However, it is not always possible to control all these factors during the synthesis of nanoparticles of approximately the same size and chemical composition, therefore, the properties of nanomaterials of the same type can vary significantly.

For the use of nanoparticles in damping devices and biomedicine, their supermagnetic state with no coercivity, i.e. zero remanent magnetization, is desirable. In this case, in their normal state, without exposure to a magnetic field, they will not form agglomerates due to attractive interaction.

It is known that the dependence of the coercive force on the particle size is complex (Fig. 1) [6]. With a decrease in the size of the bulk sample, the fraction of the surface energy of its domain borders increases, and it becomes comparable with the total volume energy. In this case, the single-domain state of a sample or particle is considered energetically more efficient. Such a state will lead to an increase in the threshold field of the remagnetization of the particle and, consequently, to an increase in the coercive force. This increase is due to a change in the remagnetization – instead of the mechanism associated with the displacement of the domain borders, the rotation of the magnetic moment vector mechanism appears. With a decrease in the size of single-domain particles, their coercive force decreases, and at a certain size its value is equal to zero. This phenomenon is explained by the influence of thermal fluctuations on the magnetic anisotropy value and, consequently, on the coercive force, since the particle anisotropy energy depends on the angle between the directions of magnetization and the easy axis of magnetization. In the superparamagnetic state, the direction of the magnetic moment vector will spontaneously change.

It is known that for isolated nanoparticles with sizes of 1–30 nm, in addition to the Curie and Neel temperatures, there is also a blocking temperature on the temperature scale: $T_B < T_C(T_N)$, where $T_C$ – Curie temperature, $T_N$ – Neel temperature $T_B$ – blocking temperature. Below the blocking temperature, the magnetic moment of the particle retains its spatial orientation, and the ensemble of particles exhibits magnetic hysteresis. At temperatures above $T_B$ the particle changes to a superparamagnetic state. In the region of $T_B < T < T_C$ the particle has spontaneous magnetization and a non-zero total magnetic moment, easily changing the orientation in an external field [7].

A characteristic problem with the production of effective nanoscale magnetic particles for MRF is their significantly lower specific magnetization compared to micron particles. This is due to a violation of the magnetic order in the subsurface layer of ~ 1 nm. In such a layer, the magnetic moments of atoms usually behave the same as

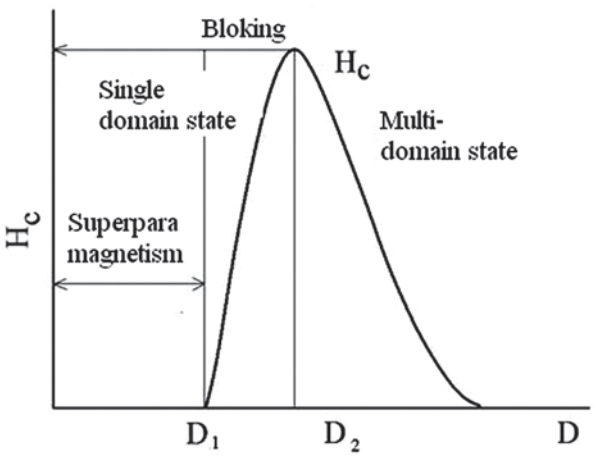


**Fig. 1.** The dependence of the coercive force on particle size

in spin glasses [8]. Therefore, there is a need to reduce the contribution of the surface layer into the specific magnetization of the material by increasing the fraction of the crystallized core of the nanoparticle. For this purpose, heat treatment is usually used, which, in turn, leads to an aggregation of particles and significant increase in their size, as well as to the appearance of residual magnetization and an increase in coercive force. Therefore, the search for new methods of influencing the microstructure of nanoobjects is relevant, for example, the use of pulsed photon processing was considered in the study [9].

The hysteretic behaviour of materials with a high coercive force in an alternating magnetic field or under dynamic shear loads leads to a decrease in their effectiveness for use in damping devices and for biomedical applications. The influence of the coercive force is particularly critical when using high-frequency fields or variable mechanical loads, when the remagnetization of particles does not have time to take effect due to the long relaxation time of magnetic properties.

Cobalt-zinc ferrites are being actively studied as promising ferrimagnetic materials with high magnetic characteristics. These materials are usually obtained by coprecipitation [10–12] or by the sol-gel method [13], electrostatic spraying [14] and other methods. The purposeful synthesis of ferrites for various applications requires information about the distribution of metal cations in the crystal lattice, since the magnetic characteristics of the samples directly depend on this distribution. Zinc ferrite has a normal crystallographic structure in accordance with the distribution of cations in the spinel sublattices, while cobalt ferrite has a reversible structure. It is known that structural deviations lead to a nonequilibrium distribution of cations in ferrites and cause a change in their magnetic properties [15, 16]. Thus, the ability to influence the cation distribution becomes a tool for tuning magnetic properties [17]. For cobalt-zinc ferrites, for example, the presence of a non-magnetic $Zn^{2+}$ ion with a strong preference for tetrahedral positions will cause the migration of $Fe^{3+}$ ions into the region of octahedral positions, leading to an increase in the magnetic moment.

We are developing dispersed ferrimagnetic nanosized particles for MRF, which, in addition to ferromagnetic particles of carbonyl iron, contains nanosized ferrimagnetic particles, allowing the enhancement of the magneto-control of damping liquids [1, 2]. Cobalt-zinc ferrite nanopowders were chosen as such particles and the analysis of their characteristics was carried out in this work. The aim of the work was the investigation of the structure, morphology, and magnetic properties of Co,Zn ferrite nanopowders and the evaluation of their effectiveness in magnetic fields upon the rheological properties of the developed MRF.

## 2. Experimental

Based on the highest specific magnetization the optimal composition of Co,Zn ferrite with a molar ratio (cobalt and zinc) of 0.65:0.35 was established [18].

Samples of $CoSO_4 \cdot 7H_2O$ weighing 16.25 g, $ZnCl_2$ weighing 4.26 g, and Fe $(NO_3)_3$ weighing 49.81 g were dissolved in 1.5 l of distilled water. The solution was stirred with magnetic stirrer for 5 min to obtain complete homogenization. An ammonia solution was poured into the resulting salt solution with vigorous stirring and the pH level was monitored to ensure it remained at 11 using indicator paper. The suspension was heated to 90 °C. The precipitate was washed by magnetic decantation, after which the aqueous suspension consisting of the precipitate of the previous stage and a NaCl solution in a mass ratio (precipitate - salt) 1: 5 was prepared.

The cobalt-zinc ferrite nanopowder was obtained by spray-drying technique. The suspension was sprayed at a temperature of 220 °C with a feed rate of 2.5 ml/min with subsequent high-temperature heat treatment in the presence of an unreacted inert matrix (NaCl), preventing the intensive growth of crystallites during heat treatment. Heat treatment was carried out in air at 740 °C for 8 h. The spray-drying method allowed obtaining micro-fine particles of salts and the products of their decomposition (100–300 °C). Subsequent annealing of such a product together with NaCl leads to the formation of the Co,Zn ferrite phase. Non-agglomerated micro-fine magnetic cobalt zinc ferrite particles are formed subsequently after the removal of the matrix (NaCl) by dissolution.

X-ray studies were performed using a DRON-3 diffractometer (Co-$K_{\alpha 1}$-radiation, λ = 0.179026 nm). Scanning was carried out in the range of angles 2θ = 6–90°. The sizes of coherent scattering regions (CSR) corresponding to the physical sizes of crystallites in polycrystalline samples were determined by the broadening of diffraction reflections (Scherrer method).

Crystal density was calculated using the formula:

$$d_x = \frac{8M}{a^3 N_A}, \quad (1)$$

where $M$ – formal molecular weight; $a$ – the lattice parameter, Å; $N_A$ – Avogadro number.

The degree of crystallinity of the samples was determined using the ratio:

$$\left(1 - \frac{I_b}{I_{311}}\right) \times 100\,\%, \quad (2)$$

where $I_{311}$ – the reflex intensity for the spinel, corresponding to the crystallographic direction 311; $I_b$ - the intensity of the spectrum background line of the x-ray diffraction pattern.

Dislocation density δ (number of lines per 1 m$^2$) was calculating using the formula:

$$\delta = \frac{1}{D^2}. \quad (3)$$

Scanning electron microscopy was used to study the surface structure of polycrystalline and film samples by use of a LEO 1420. Simultaneously the ratio of the concentration of metal atoms in ferrite powders and the features of their distribution on the surface of the particles were determined by energy dispersive x-ray spectroscopy (EDX-analysis).

IR-spectra were recorded using an AVATAR 330 spectrometer (Thermo Nicolet) in the wavenumber region (ν) 400–700 cm$^{-1}$ with an accuracy of ± 1 cm$^{-1}$. Recording was performed by diffusion reflection using the Smart Diffuse Reflectance accessory.

The magnetic characteristics were studied using a Cryogen Free Measurement System from Cryogenic Ltd, where hysteresis loops were recorded at temperatures of 2 and 300 K and magnetic field induction $B_{max}$ = 8 T. The weight of the sample, not including the capsule, was 0.09 g.

The dependence of the shear stress (τ) of the suspensions on the magnetic induction of the applied magnetic field was measured using a Physica MCR 301 Anton Paar rotational viscometer in constant shear rate mode (Mobil 22 binder, shear rate γ = 200 s$^{-1}$, $T$ = 20 °C). Powder suspensions in a binder were prepared using a UZDM–2 ultrasonic dispersant with a frequency of 44 kHz.

## 3. Results and discussion

The choice of heat treatment conditions was determined by the search for the optimal combination of the solid-phase reaction time and relative heat treatment temperature for the prevention of excessive crystallite growth.

Fig. 2 represents TEM-images of the heat treatment product of the dried precursor suspensionin NaCl solution after heat treatment at 740 °C (8 h), before (Fig. 2a) and after (Fig. 2b) washing away the NaCl. Before washing, the product was represented by spheres, sometimes of irregular shape, hollow inside and consisting of agglomerated particles of the precursor solid phase and NaCl. The sizes of these particles were in the range of 0.5–0.9 μm. The size of the spheres was 1.5–3.5 μm. The spheres were a product obtained by drying the drops formed by spraying a precursor suspension. The water, as a result of evaporation, shifted the solid phase of the precursor to the surface of the drops, where a solid shell formed with the release of volume inside the spheres. Holes caused by the release of water vapour appeared in some places on the spheres.

After dissolving sodium chloride in water, the dried $Co_{0.65}Zn_{0.35}Fe_2O_4$ powder consisted of non-agglomerated particles with sizes up to 50 nm. TEM-images of $Co_{0.65}Zn_{0.35}Fe_2O_4$ showed that the particles were well separated from each other and not agglomerated. The average particle sizes were 25–30 nm and they were comparable with the CSR size, calculated according to x-ray phase analysis (Table 1). The shape of the particles was faceted in contrast to particles obtained using other production methods for Co, Zn-ferrite nanopowders under similar temperature conditions. The result was due to the use of the synthesis of individual particles in an inert NaCl matrix, provided by the proposed method.

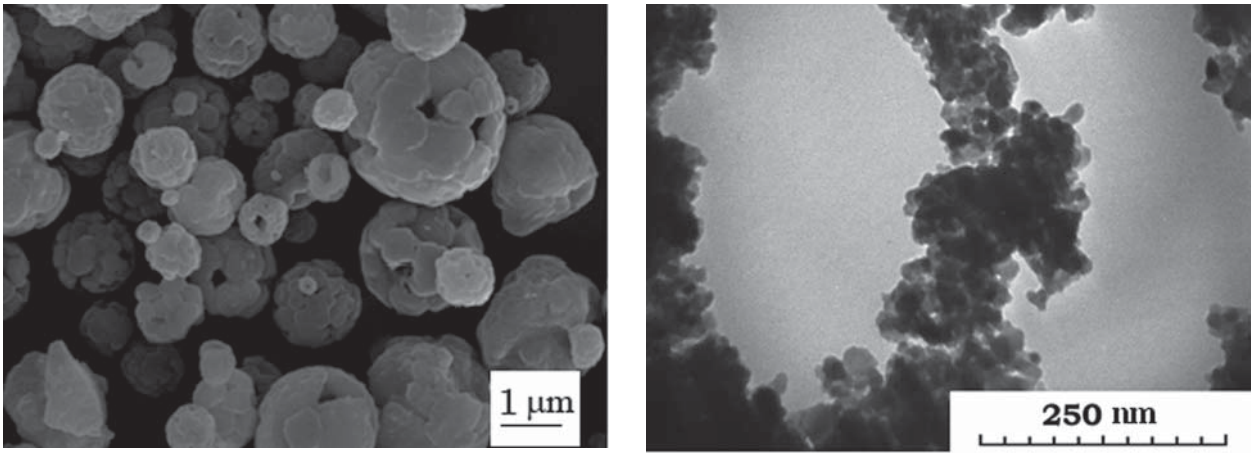


*a* *b*

**Fig. 2.** a) SEM images of $Co_{0.65}Zn_{0.35}Fe_2O_4$ particles in the NaCl matrix after heat treatment at 740 °C (8 h); b) TEM images of $Co_{0.65}Zn_{0.35}Fe_2O_4$ particles after washing away the NaCl)

Fig. 3 demonstrates typical x-ray diffraction patterns of the material obtained after heat treatment. It can be seen that after 8 h of heat treatment at a temperature of 740 °C, the solid-phase reaction with the formation of the spinel ferrite structure (space group Fd3m) was completed. Reflex positions and their relative intensities confirm that the powders represent only one phase with a spinel structure. The structural parameters of the crystal lattice of $Co_{0.65}Zn_{0.35}Fe_2O_4$ solid solution heat treated at 740 °C (8 h) are shown in Table 1. The composition of the nanoparticles was determined by energy dispersive x-ray

**Table 1.** The structural parameters of the crystal lattice of $Co_{0.65}Zn_{0.35}Fe_2O_4$ solid solution: (lattice constant *a*, size of the coherent scattering region *D*, dislocation density δ, crystal density $d_{x,}$ crystallinity)

| Lattice constant *a*, Å | Size of coherent scattering region *D*, nm | Dislocation density $\delta \times 10^2$ nm$^{-2}$ | x-ray density $d_x$, g/cm$^3$ | The degree of crystallinity, % |
|---|---|---|---|---|
| 8.3998 | 20 | 0.26 | 5.31 | 84.5 |

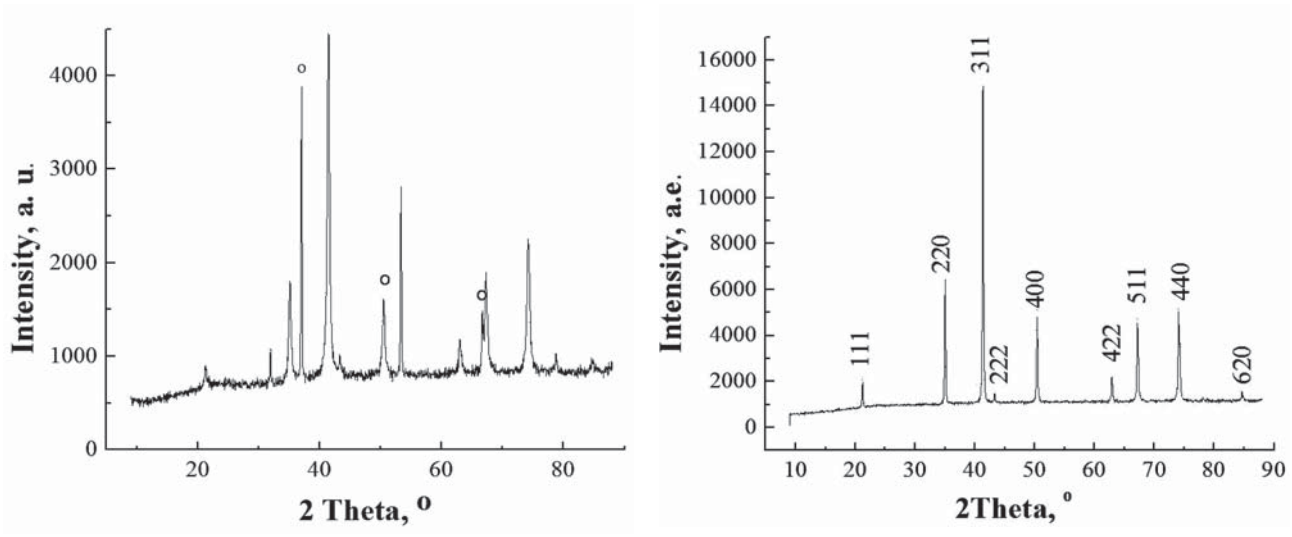


*a* *b*

**Fig. 3.** X-ray powder diffraction spectra of powders of $Co_{0.65}Zn_{0.35}Fe_2O_4$ solid solution, after heat treatment at 740 °C: a) for 2 hours; b) for 8 hours (reflexes related to $Fe_2O_3$ are marked with •)

spectroscopy. Intensive reflections related to the $\alpha$-$Fe_2O_3$ phase (haematite) were still detected after 2 h of heat treatment.

Fig. 4 represents a typical IR -absorption spectrum for $Co_{0.65}Zn_{0.35}Fe_2O_4$ nanopowders after heat treatment.

The formation of the spinel structure of ferrites was evidenced by two main absorption bands, which were combined vibrational bands of Me–O bonds in the region of characteristic frequencies with extrema at 414 and 567 $cm^{-1}$. First $\nu_1$ usually refers to the octahedral vibrations of the metal $Me_{octa} \leftrightarrow O$, and the $\nu_2$ band at 567 $cm^{-1}$ corresponds to the internal stretching vibrations of the metal in the tetrahedral site $Me_{tetra} \leftrightarrow O$ [12]. A high degree of resolution of the absorption bands may reflect a high ordering of the crystalline structure of the solid solution.

It is known that the absorption bands at $\nu_4$ = 1600 $cm^{-1}$ correspond to vibrations of adsorbed water [17]. The absorption near 2100–2300 $cm^{-1}$ may be associated with $CO_2$ adsorbed from air, absorption bands in the range of 1500–1600 $cm^{-1}$ may be associated with the vibrational oscillations of the N=O bond. Weak absorption bands near 1000 $cm^{-1}$ were due to the presence of traces of nitrate-ions [11]. Absorption bands near wave numbers 1640 and 3400 $cm^{-1}$ are associated with vibrations of O–H bonds [12]. Thus, the IR-spectrum of the sample confirms the formation of the cobalt-zinc ferrite phase and the presence of water in the material structure.

Fig. 5 shows the change in magnetization for $Co_{0.65}Zn_{0.35}Fe_2O_4$ nanopowders depending on the applied field. All prepared samples exhibited ferrimagnetic behaviour at room temperature. The obtained values of specific magnetization powder for $Co_{0.65}Zn_{0.35}Fe_2O_4$ coincided with the specific magnetization of cobalt-zinc ferrites of the same composition obtained by other methods, for example, by coprecipitation of inorganic salts from aqueous solutions (40–70 $A{\cdot}m^2{\cdot}kg^{-1}$, [19]), sol-gel method (60–80 $A{\cdot}m^2{\cdot}kg^{-1}$ [20], 60–90 $A{\cdot}m^2{\cdot}kg^{-1}$, [21]).

We demonstrated that with an increase in the zinc content in the cobalt-zinc ferrite, an increase in the saturation magnetization was noted. Thus, for $Co_{0.65}Zn_{0.35}Fe_2O_4$ *Ms* = 42.6 $A{\cdot}m^2{\cdot}kg^{-1}$, but for $CoFe_2O_4$ *Ms* = 25.0–26.0 $A{\cdot}m^2{\cdot}kg^{-1}$.

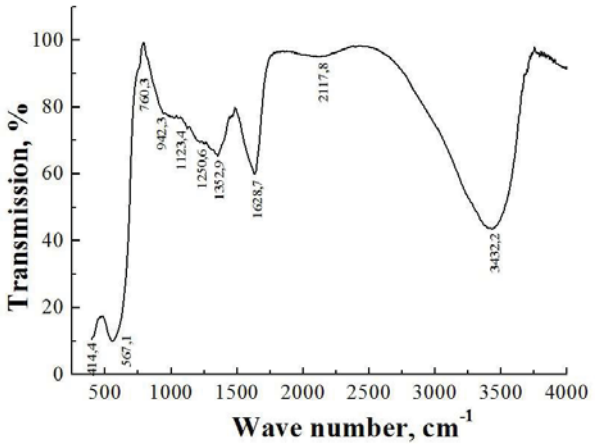


**Fig. 4.** IR absorption spectrum of $Co_{0.65}Zn_{0.35}Fe_2O_4$ after heat treatment at 740 °C for 8 h

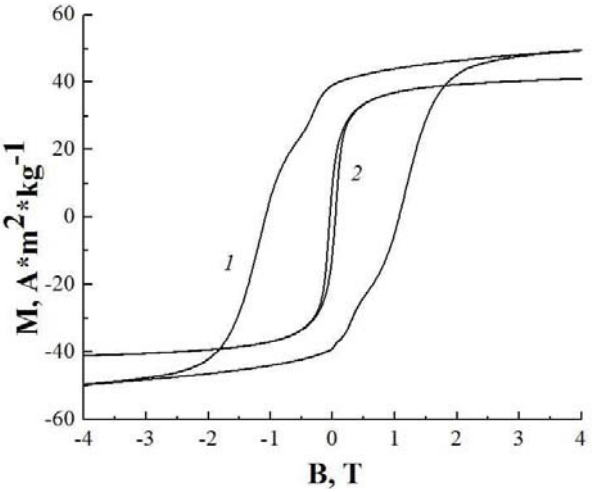


**Fig. 5.** Curves of the dependence of magnetization on magnetic field strength for $Co_{0.65}Zn_{0.35}Fe_2O_4$ powder at various temperatures of *1* - 10 K, *2* - 300 K

The magnetic ordering is associated with superexchange interaction between the ions of the octahedral (B) and tetrahedral (A) sublattices of the crystal structure for ferrimagnetic spinel ferrites.

*JAB, JBB* and *JAA* exchange integrals are usually negative and the antiferromagnetic A–B interaction is stronger than B–B and A–A interactions. This leads to ferrimagnetism of the compound, while B–B and A–A interactions are suppressed. The spins of magnetic ions will be parallel in each of the individual B–B and A–A sublattices, but in two different sublattices they are antiparallel.

As $Zn^{2+}$ ion substitutes $Co^{2+}$ ion, it pushes out $Fe^{3+}$ ions from tetrahedral A-positions into octahedral B-positions. While the magnetic

moment of A sublattice decreases due to an increased number of nonmagnetic $Zn^{2+}$ ions in it, the magnetic moment of B sublattice increases due to an increased number of Fe ions$^{3+}$ in the B sublattice. Therefore, when in the present work the concentration of $Zn^{2+}$ ions increased from 0 to 0.35, the total magnetization ($M_{oct}$ – $M_{tet}$) for $Co_{1-x}Zn_xFe_2O_4$ also increased due to an increase in interlattice A–B superexchange interactions between the magnetic ions of A and B sublattices. Magnetic moments of $Fe^{3+}$ ions in different sublattices of the crystal spinel structure (octahedral and tetrahedral) will not be mutually compensated as before.

However, at high levels of doping with $Zn^{2+}$ ions ($x > 0.35$) the antiferromagnetic interaction of $Fe^{3+}$ ions located in neighbouring positions in the octahedral sublattice begins. It turned out that the B–B interaction leads to a decrease in the total magnetic moment.

The explanation for this phenomenon is provided by the three-sublattice Yafet–Kittel model [22], demonstrating that with an increase in the B–B interaction, the A–B interaction decreases. When exchange interactions appear in a ferrimagnet inside B–B or A–A sublattices, they already start "competing" with the interlattice A–B interaction. Most likely, the reason for such an increase in the interaction in the B or A sublattices is the appearance of noncollinearity of spins in the sublattice, leading to a decrease in the values of the experimental magnetic moment.

According to the two-sublattice Neel model of ferromagnetism, the theoretical magnetic moment $\mu_B$ per formula unit in $n_B^t$ is described as

$$n_B^m(x) = M_B(x) - M_A(x), \quad (4)$$

Where $M_B(x)$ and $M_A(x)$ are the magnetic moments of the B and A sublattice in $\mu_B$respectively. The distribution of cations in $Co_{1-x}Zn_xFe_2O_4$ can be written as

$$(Zn_x^{2+}\,Fe_{1-x}^{3+})_A[Co_{1-x}^{2+}\,Fe_{1+x}^{3+}]_B\,O_4^{2-}. \quad (5)$$

Depending on the concentration of Zn, the theoretical values of the magnetic moment, $n_B^T$ in $Co_{1-x}Zn_xFe_2O_4$ are calculated using the distribution of cations and magnetic moments of $Fe^{3+}$, $Co^{2+}$ and $Zn^{2+}$ ions, equal to 4.85 $\mu_B$, 2.78 $\mu_B$ and 0 $\mu_B$, respectively. Experimental values of magnetic moments ($n_B^e$), per unit of the formula in Bohr magnetrons ($\mu_B$), were calculated according to the ratio:

$$n_B^e = \frac{M_w M_s}{5585}, \quad (6)$$

where $M_w$ – molecular weight, $M_s$ – saturation magnetization, and 5585 – magnetic factor [22].

It turned out that the theoretical magnetic moment increases linearly as a function of $Zn^{2+}$ concentration, and the experimental magnetic moment increases with the concentration of $Zn^{2+}$ in $Co_{0.65}Zn_{0.35}Fe_2O_4$ before $x = 0.35$, and then gradually decreases. For $Co_{0.65}Zn_{0.35}Fe_2O_4$composition $n_B^T = 4.95\ \mu_B$, and $n_B^E = 3.01\ \mu_B$.

The values of the magnetic parameters obtained for the hysteresis loops are summarized in Table 2.

**Table 2.** The parameters of the magnetization curves of $Co_{0.65}Zn_{0.35}Fe_2O_4$ particles (saturation magnetization $M_s$, adjusted remanent magnetization $M_r/M_s$, coercive force $H_c$)

| $T$, K | $M_s$, Am$^2$·kg$^{-1}$ | $M_r/M_s$ | $H_c$, kOe |
|---|---|---|---|
| 10 | 52.47 | 0.75 | 10.9 |
| 50 | 52.42 | 0.72 | 9.0 |
| 100 | 51.67 | 0.67 | 5.9 |
| 200 | 48.09 | 0.47 | 1.7 |
| 300 | 42.57 | 0.24 | 0.46 |

It was established that in terms of shape they are close to the known literature data for cobalt ferrite and are characterized by their significant rectangularity, which is reflected in the values of the adjusted remanent magnetization [23]. Saturation magnetization values $M_s$ in the range of 5–300 K were slightly reduced. High values ofadjusted remanent magnetization can be associated with monodispersity of particles. Magnetization $M_s$ values slightly decreased with a temperature increase in the range of 10–300 K, while the adjusted remanent magnetization $M_r/M_s$ ($M_r$ – residual induction $M_s$ – saturation induction) and coercive force $H_c$ values decreased significantly with the temperature increase, due to the influence of thermal fluctuations of the magnetization of individual particles [24].

It is known, that coercivity is associated with the characteristic constant of the material anisotropy. At the nanoscale, anisotropy depends on various factors, such as particle size, exchange biases, dipole interactions, particle shape, and crystalline nature. The comparison of $H_c$ for the

obtained Co,Zn-nanoferrite, with the magnetic properties of cobalt nanoferrite demonstrated a significant decrease of $H_c$ upon the doping of Co,Zn-ferrite with zinc. For example, at 300 K, the coercive force for our $Co_{0.65}Zn_{0.35}Fe_2O_4$ sample was 2.5 times lower than for $CoFe_2O_4$ at the same particle sizes [13]. We obtained the same results for nanopowders synthesized by aerosol pyrolysis with the same heat treatment as for spray-drying technique. For $Co_{0.65}Zn_{0.35}Fe_2O_4$ $H_c$ = 0.13 kOe, and $CoFe_2O_4H_c$ = 0.37 kOe [25]. Thus, for the synthesized Co,Zn ferrite nanoparticles, the substitution of cobalt atoms by zinc led to a decrease in anisotropy and, consequently, a decrease in the coercive force.

The adjusted residual magnetization ($M_r/M_s$) values of $Co_{0.65}Zn_{0.35}Fe_2O_4$ at different temperatures are presented in Table 2. It was found that they gradually decrease for higher temperatures. The Stoner-Wohlfarth model determines that for low temperatures $M_r/M_S$ = 0.5 for randomly oriented uniaxial noninteracting particles ensembles and when the anisotropy of disordered and noninteracting nanoparticles is cubic, then $M_r/M_s$= 0.83. In our case, for $Co_{0.65}Zn_{0.35}Fe_2O_4$ samples at temperatures below 200 K, $M_r/M_s$ is definitely higher than 0.5 and cubic anisotropy is more pronounced here. These results show that coercivity can be regulated and changed in the structure of Co, Zn-spinels by replacing cobalt ions with zinc ions.

On the hysteresis loop at low temperatures (Fig. 5) we also observed a distortion in the curve of the dependence of the magnetization on the field strength next to the residual magnetization in the form of unusual bends. The existence of such bends is associated with the two-phase behaviour of the hysteresis loop, interparticle interactions, etc. [26, 27]. It also seems that there is an interaction between the hard and soft anisotropy regimes. In addition, this phenomenon may depend on the polydispersity of the sizes, as well as on the shape of the particles.

The dependences of the shear stress of an MRF containing 20 wt.% $Co_{0.65}Zn_{0.35}Fe_2O_4$ powder, on shear rate in the absence of a magnetic field and on magnetic field induction at a shear rate of 200 $s^{-1}$, $T$ = 20 °C were measured for the assessment of the effectiveness of the synthesized particles (Fig. 6). A high value of shear stress (1000 Pa) at relatively low values of the magnetic field induction (from 600 mT and above) allowed considering the obtained material to be suitable for practical use as a component of MRF filler. It is known that ferrimagnetic powders with a large value of the residual magnetization can exhibit a significantly lower increase in viscosity in a magnetic field. Thus, for example, zinc-containing an iron oxide powder at $M_s$ (300 K) = 95 $A \cdot m^2 \cdot kg^{-1}$ exhibits insignificant viscosity change in a magnetic field (about 15 %) [1].

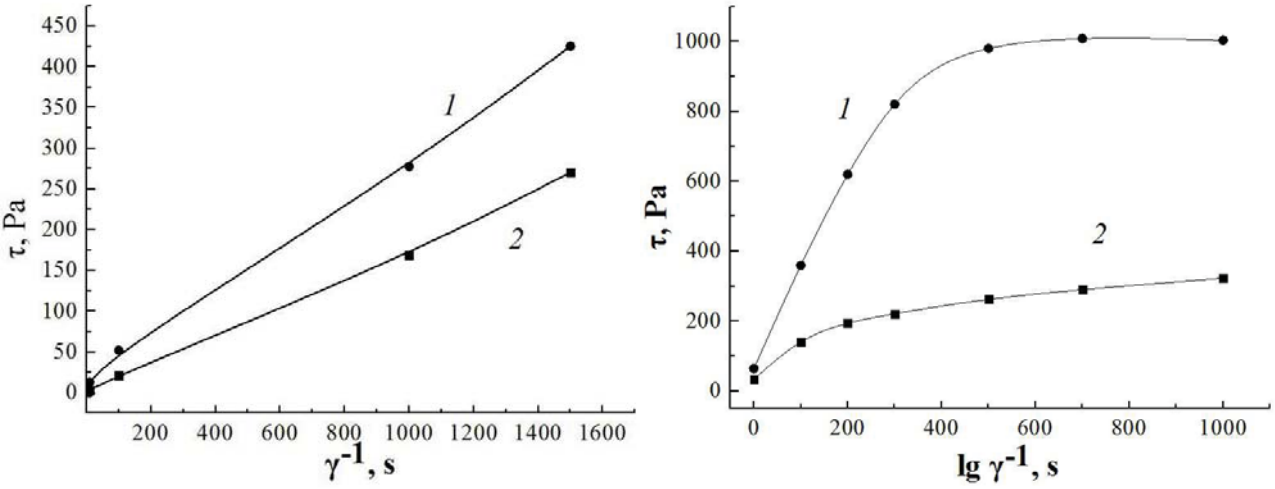


*a* *b*

**Fig. 6.** The dependence of the shear stress of an MRF containing 20 wt.% magnetic nanoparticles *1* – $Co_{0.65}Zn_{0.35}Fe_2O_4$; *2* – $Mn_{0.3}Fe_{2.7}O_4$ in Mobil 22 oil: a) on shear rate in the absence of a magnetic field; b) in a magnetic field at shear rate γ = 200 $s^{-1}$, $T$ = 20 ˚C

From the dependence of the shear stress of a suspension prepared based on $Co_{0.65}Zn_{0.35}Fe_2O_4$ powder, it is also seen that the shear stress of the suspension increased with increased magnetic field induction and reached a maximum value of 1 kPa at 550 mT, which is significantly lower than for most other known materials based on doped magnetites and ferrites. In addition, $Co_{0.65}Zn_{0.35}Fe_2O_4$ powders have high oil absorption and form stable suspensions. This allows using them as a stabilizing and modifying filler in magnetorheological suspensions based on carbonyl iron in synthetic oil.

## 4. Conclusions

A technique has been developed that allows controlling the magnetic properties of cobalt-zinc ferrite as a component of magnetorheological suspensions by non-magnetic double charge ion substitution of cobalt ions, i. e. zinc ionsin the structure of Co,Zn spinel. The possibility to decrease the coercive force and increase magnetization up to maximum cobalt content corresponding to the composition formulae $Co_{0.65}Zn_{0.35}Fe_2O_4$ has been established. For the synthesis of cobalt-zinc ferrite, a spray-drying technique followed by heat treatment in the inert component NaCl matrix has been proposed. The proposed technique allows obtaining uniform crystallized cobalt-zinc ferrite nanoparticles with a diameter less than 50 nm, with a specific magnetization of about ~ 40 $A{\cdot}m^2{\cdot}kg^{-1}$, some of which were in a superparamagnetic state. The efficiency of $Co_{0.65}Zn_{0.35}Fe_2O_4$ in MRF composition with the industrial Mobil 22 oil (20% wt.) has been assessed, the dependence of the shear stress on the induction of the magnetic field was investigated. The high shear stress (1 kPa) with a relatively low magnetic field induction (from 600 mT and above) allowed us to consider the obtained material as being promising for use as an additional functional filler for the magnetorheological suspensions of damping devices.

## Conflict of interests

The authors declare that they have no known competing financial interests or personal relationships that could have influenced the work reported in this paper.

## References

1. Korobko E. V., Pankov V. V., Kotikov D. A., Novikova Z. A., Novik E. S. Nanodispersed fillers based on iron oxide for the complex dispersed phase of magnetically correctable hydraulic fluids. In: *Nanostructures in condensed matter: Collection of scientific articles, 20–23 August* 2018. Minsk: A. V. Lykov Heat and Mass Transfer Institute National Academy of Sciences of Belarus Publ.; 2018. p. 156–161. (In Russ.)

2. Dragašius E., Korobko E., Novikava Z., Sermyazhko E. Magnetosensitive Polymer composites and effect of magnetic field directivity on their properties. *Solid State Phenomena*. 2016;251: 3–7. DOI: https://doi.org/10.4028/www.scientific.net/SSP.251.3

3. Joseph A., Mathew S. Ferrofluids: synthetic strategies, stabilization, physicochemical features, characterization, and applications. *ChemPlusChem*. 2014;79(10):1382–1420. DOI: https://doi.org/10.1002/cplu.201402202

4. Genc S., Derin B. Synthesis and rheology of ferrofluids: a review. *Current Opinion in Chemical Engeeniring*. 2014;3(2): 118–124. DOI: https://doi.org/10.1016/j.coche.2013.12.006

5. Vekas L., Avdeev M. V., Bica D. Magnetic nanofluids: synthesis and structure. In: Donglu Shi (ed.) *Nanoscience in biomedicine*. Springer Berlin Heidelberg; 2009. 729 p. DOI: https://doi.org/10.1007/978-3-540-49661-8

6. Frolov G. I., Bachina O. I., Zav'yalova M. M., Ravochkin S. I. Magnetic properties of nanoparticles of 3D metals. *Technical physics*. 2008;53(8):1059–1064. DOI: https://doi.org/10.1134/S1063784208080136

7. Baraton M. I. Synthesis, functionalization, and surface treatment of nanoparticles, LA: Am. Sci. Publ.; 2002. 236 p.

8. Martínez B., Obradors X., Balcells L., Rouanet A., Monty C. Effect of aluminum doping on structural and magnetic properties of Ni Zn ferrite nanoparticles. *Physical Review Letters*. 1998;80(1): 181–184. DOI: https://doi.org/10.4236/wjnse.2015.53009

9. Mittova I. Ya., Sladkopevtsev B. V., Mittova V. O., Nguyen Anh Tien, Kopeichenko E. I., Khoroshikh N. V., Varnachkina I. A. Formation of nanoscale films of the ($Y_2O_3$–$Fe_2O_3$) on the monocrystal InP. *Kondensirovannye sredy i mezhfaznye granitsy = Condensed Matter and Interphases*. 2019;21 (3): 406–418. DOI: 10.17308/kcmf.2019.21/1156 (In Russ., Abstract in Eng.)

10. Mayekar J., Dhar V., Radha S. Synthesis, characterization and magnetic study of zinc ferrite nanoparticles. *International Journal of Innovative Research in Science, Engineering and Technology*. 2016;5(5): 8367–8371. DOI: https://doi.org/10.15680/IJIRSET.2016.0505268

11. Jansi Rani B., Ravina M., Saravanakumar B., Ravi G., Ganesh V., Ravichandran S., Yuvakkumar R. Ferrimagnetism in cobalt ferrite ($CoFe_2O_4$) nanoparticles. *Nano-Structures & Nano-Objects*. 2018;14: 84–91. DOI: https://doi.org/10.1016/j.nanoso.2018.01.012

12. Manouchehri S., Ghasemian Z., Shahbazi-Gahrouei D., Abdolah M. Synthesis and characterization of cobalt-zinc ferrite nanoparticles coated with DMSA. *Chem Xpress*. 2013;2(3): 147–152.

13. Singhal S., Namgyal T., Bansal S., Chandra K. Effect of Zn Substitution on the magnetic properties of cobalt ferrite nanoparticles prepared via sol-gel route. *Journal of Electromagnetic Analysis and Applications*. 2010;2(6): 376–381. DOI: https://doi.org/10.4236/jemaa.2010.26049

14. Rajendra S. G., Sang-Youn Ch., Rajaram S. M., Sung-Hwan H., Oh-Shim J. Cobalt ferrite nanocrystallites for sustainable hydrogen production application. *International Journal of Electrochemistry*. 2011;2011: 1–6. DOI: https://doi.org/10.4061/2011/729141

15. Ladole C. A.Preparation and characterization of spinel zinc ferrite $ZnFe_2O_4$. *International Journal of Chemical Science*. 2012;10(3): 1230–1234. Available at: https://www.tsijournals.com/articles/preparation-and-characterization-of-spinel-zinc-ferrite-znfe2o4.pdf

16. Raghuvanshi S., Kane S. N., Tatarchuk T. R., Mazaleyrat F. Effect of Zn addition on structural, magnetic properties, antistructuralmodeling of $Co_{1-x}Zn_xFe_2O_4$nanoferrite. *AIP Conference Proceedings*. 2018;1953(1): 030055. DOI: https://doi.org/10.1063/1.5032390

17. Sawadzky G. A., Van der Woude F., Morrish A. H. Cation distributions in octahedral and tetrahedral sites of the ferrimagnetic spinel $CoFe_2O_4$. *Journal of Applied Physics*. 1968;39(2): 1204–1206. DOI: https://doi.org/10.1063/1.1656224

18. Petrova E. G., ShavshukovaYa. A., Kotikov D. A., Yanushkevich K. I., Laznev K. V., Pan'kov V. V. Thermolysis of sprayed suspensions for obtaining highly spinel ferrite nanoparticles. *Journal of the Belarusian State University. Chemistry*. 2019;1: 14–21. Available at: https://journals.bsu.by/index.php/chemistry/article/view/1258 (In Russ., abstract in Eng.)

19. Ranjani M., Jesurani S., Priyadharshini M., Vennila S. Sol-gel synthesis and characterization of zinc substituted cobalt ferrite magnetic nanoparticles. *International Journal of Advanced Research*. 2016;4(7): 53–58. DOI: https://doi.org/10.21474/ijar01/1148

20. Lin Q., Xu J., Yang F., Lin J., Yang H., He Y. Magnetic and mцssbauer spectroscopy studies of zinc-substituted cobalt ferrites prepared by the sol-gel method. *Materials*. 2018;11(10): 1799. DOI: https://doi.org/10.3390/ma11101799

21. Copolla P., da Silva F. G., Gomide G., Paula F. L. O, Campos A. F. C., Perzynski R., Kern C., Depeyrot G., Aquino R. Hydrothermal synthesis of mixed zinc–cobalt ferrite nanoparticles: structural and magnetic properties. *Journal of Nanoparticle Research*. 2016;18(138): 1–15. DOI: https://doi.org/10.1007/s11051-016-3430-1

22. Yafet Y., Kittel C. Antiferromagnetic arrangements in ferrites. *Physical Review Journal*. 1952;87(2): 290–294. DOI: https://doi.org/10.1103/PhysRev.87.290

23. Praveena K., Sadhana K. Ferromagnetic properties of Zn substituted spinel ferrites for high frequency applications. *International Journal of Scientific and Research Publications*. 2015;5(4): 1–21. Available at: http://www.ijsrp.org/research-paper-0415.php?rp=P403877

24. Komogortsev S. V., Patrusheva T. N., Balaev D. A., Denisova E. A., Ponomarenko I. V. Cobalt ferrite nanoparticles in a mesoporous silicon dioxide matrix. *Technical Physics Letters*. 2009;35(19): 882–884. DOI: https://doi.org/10.1134/S1063785009100022

25. Komogortsev S. V., Iskhakov R. S., Balaev A. D., Kudashov A. G., Okotrub A. V., Smirnov S. I. Magnetic properties of Fe3C ferromagnetic nanoparticles encapsulated in carbon nanotubes. *Physics of the Solid State*. 2007;49(4): 734–738. DOI: https://doi.org/10.1134/S1063783407040233

26. Ivashenko D. V., Petrova E. G., Mittova I. Ya., Ivanets A. I., Pankov V. V. Synthesis of cobalt-zinc ferrite nanoparticles by modified aerosol pyrolysis. In: *Alternative Sources of Raw Materials and Fuels*: *Materials of the VII International Scientific and Technical Conference, 28–30 May 2019*. Minsk: 2019. p. 120. Available at: http://aist.ichnm.by/doc/Abstract_AICT_2019.pdf (In Russ.)

27. Gözüak, F., Koseoglu, Y., Baykal, A., Kavas H. Synthesis and characterization of $Co_xZn_{1-x}Fe_2O_4$ magnetic nanoparticles via a PEG-assisted route. *Journal of Magnetism and Magnetic Materials*. 2009;321(14): 2170–2177. DOI: https://doi.org/10.1016/j.jmmm.2009.01.008

28. Abdallah H. M. I., Moyo T., Ezekiel I. P., Osman N. S. E. Structural and magnetic properties of $Sr_{0.5}Co_{0.5}Fe_2O_4$ nanoferrite. *Journal of Magnetism and Magnetic Materials*. 2014;365(9): 83–87. DOI: https://doi.org/10.1016/j.jmmm.2014.04.041

## Information about the authors

*Yulyan S. Haiduk*, Researcher, Belarusian State University, Minsk, Republic of Belarus; e-mail: j_hajduk@bk.ru. ORCID iD: https://orcid.org/0000-0003-2737-0434.

*Evguenia V. Korobko*, DSc in Engineering, Professor, Head of Laboratory, A. V. Luikov Heat and Mass Transfer Institute of the National Academy of Sciences

of Belarus, Minsk, Belarus; e-mail: evkorobko@gmail.com. ORCID iD: https://orcid.org/0000-0002-2870-9658.

*Kristsina A. Sheutsova*, Engineer, A. V. Luikov Heat and Mass Transfer Institute of the National Academy of Sciences of Belarus, Minsk, Belarus; e-mail: kristina-shevcova@lenta.ru. ORCID iD: https://orcid.org/0000-0001-7360-5965.

*Dzmitry A. Kotsikau*, PhD in Chemistry,Associate Professor, Belarusian State University, Minsk, Belarus; e-mail: kotsikau@bsu.by. ORCID iD: https://orcid.org/0000-0002-3318-7620.

*Ivan A. Svito*, PhD in Physics and Mathematics, Senior researcher of Energy Physics Department, Belarusian State University, Minsk, Belarus; Email: ivansvito184@gmail.com. ORCID iDhttps://orcid.org/0000-0002-4510-0190.

*Alexandra E. Usenka,* PhD in Chemistry, Associate Professor, Belarusian State University, Minsk, Republic of Belarus; e-mail: usenka@bsu.by. ORCID iD: https://orcid.org/0000-0002-2251-619.

*Dzimitry U. Ivashenka*, Master of Chemistry Researcher, Belarusian State University, Minsk, Belarus; e-mail: ivashenkodm@gmail.com. ORCID ID: https://orcid.org/0000-0002-9149-7213.

*Amir Fahmi*, Doctor, Professor, University of Applied Sciences, Kleve, Germany; e-mail: Amir.Fahmi@hochschule-rhein-waal.de. ORCID iD: https://orcid.org/0000-0001-5283-4646.

*Vladimir V. Pankov*, DSc in Chemistry, Professor, Head of the Department of Physical Chemistry, Belarusian State University, Minsk, Belarus; e-mail: pankov@bsu.by. ORCID iD: https://orcid.org/0000-0001-5478-0194.

All authors have read and approved the final manuscript.

*Translated by Valentina Mittova.*
*Edited and proofread by Simon Cox.*